SOFC hybrid system optimization using an advanced model of fuel cell

J. Milewski

Abstract—The advanced mathematical model of Solid Oxide Fuel Cell (SOFC) is presented. Electrochemical, thermal, electrical and flow parameters are collected in the 0D mathematical model. The aim was to combine all cell working conditions in the lowest number of readily determined factors possible. A validation process for various experimental data was made and adequate results are shown.

The model was utilized for hybrid system parameters optimization. As a result, the optimum point of system operation is determined and commented. The influences of several factors are investigated.

Keywords—Solid Oxide Fuel Cell, Mathematical modelling

I. INTRODUCTION

AT presently, energy is produced by large power plants and distributed to customers through a national grid. In the future energy distribution will probably take a radically different form – it will be composed of numerous small units connected to a network called distribution generation (DG).

DG is a system of energy distribution where energy is produced locally. Interconnection to the grid allows energy to be bought from and sold to other customers. Energy sources for DG will have to meet certain requirements: appropriate range of power output, electric efficiency – which are higher than presently obtained by large power plants – acceptable costs of installation, possibility of utilization of standard fuels.

Most of the requirements are met by fuel cell hybrid systems (HS). Solid Oxide Fuel Cells (SOFCs) are potential sources of this system of energy conversion due to their high efficiency and ability to make direct use of hydrocarbons. Moreover, their high working temperature allows for the possibility of using lower-cost catalysts (Ni vs. Pt) and adding a gas turbine subsystem to increase total efficiency.

There are many mathematical models of the singular solid oxide fuel cell (SOFC) [1]–[3]. SOFC performance modelling is related to the multi-physic processes taking place on the fuel cell surfaces. Heat transfer together with electrochemical reactions, mass and charge transport are conducted inside the cell. The SOFC models found in the literature are based mainly on mathematical descriptions of these physical, chemical, and electrochemical properties.

The SOFC models developed thus far are mainly based on the Nernst equation, activation, ohmic, and concentration losses. Actually, this means that specific current-voltage curve is approximated by several factors like current limiting, exchange current and so forth. This approach results in good agreement with particular experimental data (for which adequate factors were obtained) and poor agreement for non-original experimental working parameters. Moreover, most of the equations require the addition of numerous factors (porosity, tortuosity, ionic and electronic paths, etc.) which are difficult to determine and which are often related to the microscopic properties of the cell which govern both chemical and electrochemical reaction. Those parameters are frequently used as fitting parameters without any physical background. This is particularly relevant in the case of complex fuel feeding. It is far from straightforward to determine all requisite coefficients and factors even for small number of current-voltage curves for hydrogen as a fuel only. Introduction of other components makes this task substantially more difficult. A new model is proposed and the governing equations of this model are presented in this paper.

II. THEORY

Mathematical modelling is now the basic method for analyzing systems incorporating fuel cells. A zero-dimensional approach is used for the modelling of system elements.

A. SOFC

The working principles of SOFC are shown in Fig. 1. The oxygen partial pressure difference between anode and cathode forces oxygen ions ($O^{=}$) to pass through the solid electrolyte. This process generates voltage and an electric current can be drawn from the cell.

The maximum voltage of the fuel cell depends on the type of reaction occurring on the electrode surfaces. The maximum

J. Milewski, Warsaw University of Technology, Institute of Heat Engineering (milewski@itc.pw.edu.pl).

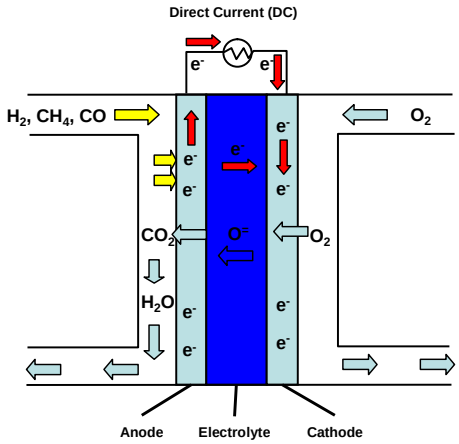

Fig. 1. Working principles of SOFC

TABLE I
MAXIMUM VOLTAGES FOR VARIOUS REACTIONS

Chamical Reaction	Maximum Voltage at 20°C
$H_2 + \frac{1}{2}O_2 \rightarrow H_2O$	1.23 V
$CH_4 + 2O_2 \rightarrow CO_2 + H_2O$	1.06
$CH_3OH + \frac{3}{2}O_2 \rightarrow CO_2 + 2H_2O$	1.22
$C + O_2 \rightarrow CO2$	1.03
$C + \frac{1}{2}O_2 \rightarrow CO$	0.72
$CO + \frac{1}{2}O_2 \rightarrow CO_2$	1.34

voltages for various reactions are listed in Table I from which it can be seen that various fuels in reaction with oxygen can give various maximum voltages. Mixtures of various components occur in the case of the analyzed fuels. Due to these circumstances the general form of Nernst's equation is used to estimate the voltage of SOFC:

$$E_{\max} = \frac{R \cdot T}{4F} \ln \frac{p_{O_2,cathode}}{p_{O_2,anode}} \tag{1}$$

where: T – abdolute temperature, R – universal gas constant, F – Faraday's constant, p – partial pressure at outlet stream.

Adequate partial pressures can be calculated based on thermodynamic functions of Peng-Robinson equation of state and minimization of Gibbs free energy [4].

The equivalent electric circuit of a singular cell is shown in Fig. 2. The total current which can be drawn from the cell is strictly correlated with the amount of fuel delivered. This means that it is a value of current for which the whole fuel is utilized - Imax. Then, the fuel utilization factor can be correlated with the current generated by the cell:

$$I_3 = (I_{\max} - I_1) \cdot \eta_f \tag{2}$$

where: η_f – fuel utilization factor.

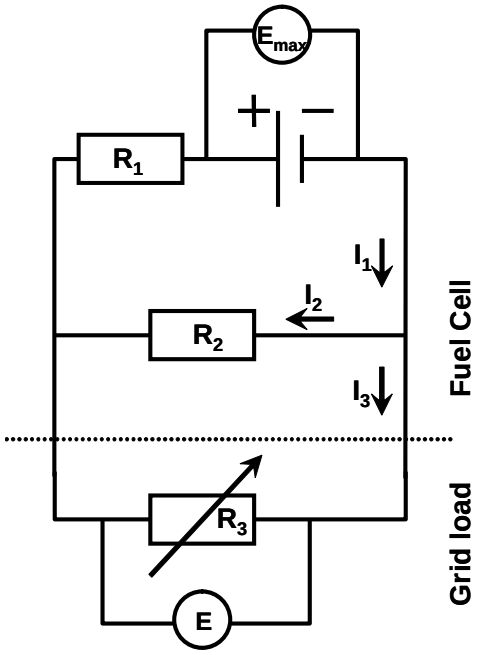

Fig. 2. Equivalent electric circuit of the cell

$$I_{\max} = 2F \cdot \dot{n}_{H_2,equivalent} \tag{3}$$

where: $\dot{n}$– molar flow.

The mixture of various fuels enters into the SOFC anode, so the fuel utilization factor is calculated based on an equivalent hydrogen molar flow.

Two types of resistance are present in fuel cells: ionic resistance r_1 and electric resistance r_2 (see Fig. 1). Resistance r_3 is the external load resistance of the fuel cell. The second resistance has meaning of electrons passing through the electrolyte layer. For the electric circuit shown in Fig. 2, using Ohm's and Kirchhoff's laws, a set of equations can be built as follows:

$$\begin{cases} E_{\max} = R_1 \cdot I_1 + R_2 \cdot I_2 \\ I_1 = I_2 + I_3 \\ E = R_2 \cdot I_2 \end{cases} \tag{4}$$

By solving both the set of Equations 2 and Equation 2 an equation for the cell voltage is obtained [5]:

$$E_{SOFC} = \frac{E_{\max} - \eta_f \cdot i_{\max} \cdot r_1}{\frac{r_1}{r_2}(1 - \eta_f) + 1} \tag{5}$$

where: $E_{\max}$ – maximum voltage; η_f – fuel utilization factor; $i_{\max}$ – maximum current density; r_1 – internal ionic area specific resistance of the cell; r_2 – internal electronic area specific resistance of the cell.

The value of maximum current density ($i_{\max}$) is constant in the design point calculations. In the case of design point calculations, the voltage-fuel utilization factor curve ($E = f(\eta_f)$) is the fuel cell characteristic. E.g. the $i_{\max}$ of 4.58A/cm^2 was determined by the researchers' own calculations, which were based on data taken from [6], [7]. This means that in design point calculations the cell area is always fixed in relation to inlet fuel flow. A lower value of the imax means a larger cell area of the fuel cell for the same fuel utilization factor.

The fuel cell characteristic is defined by a voltage-current density curve ($E = f(i)$). The area of the cell is fixed during off-design calculations, which means that factor imax has to be calculated based on the following equations:

$$i_{\max} = \frac{2F \cdot n_{H_2,equivalent}}{A} \tag{6}$$

where: A – cell area.

Area Specific Ionic Resistance: Total ionic resistance of the cell is a function of many parameters. The solid oxide fuel cell consists of electrolyte covered by anode and cathode layers. Those layers influence ionic conductivity as well (e.g. triple boundary phase processes). The material used, porosity and design of the electrodes have a significant influence on fuel cell voltage [5]:

$$r_1 = \sum \frac{\delta \cdot (1-\rho)}{\sigma} \tag{7}$$

where: δ – layer thickess, σ– layer ionic conductivity.

The ionic conductivity of the solid oxide is defined as follows:

$$\sigma = \sigma_0 \cdot e^{\frac{-E_{act}}{R \cdot T}} \tag{8}$$

where: σ_0, and E_{act} – factors dependent on material used.

The ionic resistance of solid oxides as a function of electrolyte temperature is shown in Fig. 3.

Area Specific Electric Resistance: In general, solid oxides are assumed to be only ionic conductors, but in fact electron conductivity is present as well [8]. Gas leakage through the electrolyte has the same effect as electron (electrical) conductance and can be described in the same way.

The second type of internal resistance is electric resistance– r_2 (see Fig. 2). The influences of temperature and electrolyte thickness on electronic internal resistance of electrolytes are not well known. The electronic conductivity values of solid oxide electrolytes are probably spread across a very wide range. They do not have a major impact on calculated cell voltage for high fuel utilization factors. It is difficult to measure

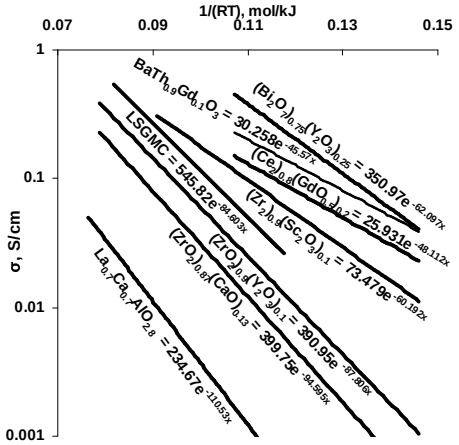

Fig. 3. Temperature dependence of ionic conductivity for solid oxides

the electronic resistance of solid oxide electrolytes since they have both conductivities–ionic and electronic–simultaneously, which gives total electrical resistance. It should be noted that decreasing electrolyte thickness reduces ionic resistance, but also probably reduces electronic resistance.

Apart from a physical explanation of the difference between calculated maximum cell voltage and related open circuit voltage, for given r_1, $E_{\max}$ and E_{OCV} (from experimental measurements) the value of electrical resistance of the cell can be found by using the following relationship:

$$r_2 = \frac{\delta}{\sigma_2} \tag{9}$$

The value of electrical resistance of the cell can be estimated from available experimental results. Substituting $\eta_f = 0$ into Eq. 5, the E_{OCV} can be defined by the following relationship:

$$E_{SOFC} = \frac{E_{\max}}{\frac{r_1}{r_2} + 1} \tag{10}$$

Substituting Eq. 9 into Eq. 10, the relationship for electrical conductivity of the cell is obtained:

$$\sigma_2 = \delta \frac{E_{\max} - E_{OCV}}{r_1 \cdot E_{OCV}} \tag{11}$$

The electrical conductivities of solid oxides were estimated by using Eq. 11 and based on experimental data published in [9]–[16]. The result of this estimation is shown in Fig. 4.

Model validation: Experimental data published in [6] were used to model validation (see Fig. .5). The tested cell has an area of 1.1 cm², and the following oxidant and fuel flows were kept constant: oxidant 550 ml/min and fuel 140 ml/min, respectively. The cell was tested at a constant temperature of 800°C.

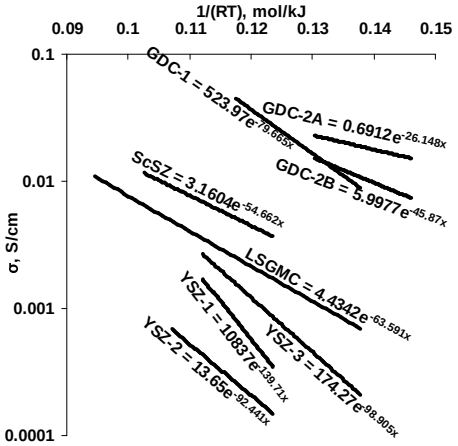

Fig. 4. Temperature dependence of electrical conductivity for solid oxides

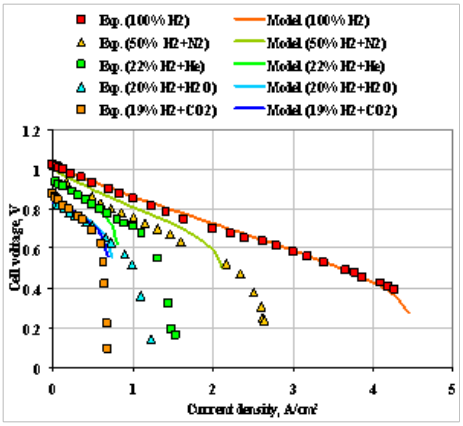

Fig. 5. Experimental and simulation data at various fuel compositions for experimental data taken from [6]. Temperature 800°C, air as oxidant

The tested cell was constructed of YSZ-SDC bilayer electrolyte supported by the anode layer. The thickness of the SDC layer was around 3 µm and the total thickness of the YSZ-SDC bilayer electrolyte thin film was 10 µm. Then, the ionic resistance of the fuel cell was calculated as follows:

$$r_1 = \frac{\delta_{SDC}}{\sigma_{SDC}} + \frac{\delta_{YSZ}}{\sigma_{YSZ}} + r_{electrodes} \tag{12}$$

Adequate factors of ionic conductivity for both layers were read from Fig. 3, whereas resistance of the electrodes was fitted (in fact there is only one fitting parameter in the model) and assumed constant: 0.06 cm²/S. It should be noted that electrode losses are significant (62%) at 800°C compared with electrolyte losses. Often, both anode and cathode layers contain the same material which is used for electrolyte. It is evident that temperature has a significant influence. Further work will focus on finding adequate relationships for that.

Voltages and current densities ware calculated based on equations presented in this paper. The model was compared

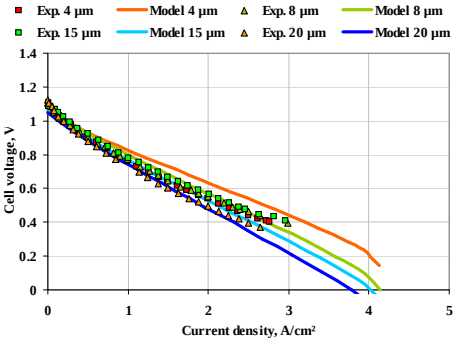

Fig. 6. Experimental and simulations data at various electrolyte thicknesses (experimental data taken from [7])

with experimental data for hydrogen as a fuel diluted by helium and hydrogen as a fuel diluted with steam; this comparison is shown in Fig. 5.

SOFC fuelled by dry hydrogen is modelled with higher accuracy than other fuel compositions. Lower hydrogen content in the fuel mixture is modelled with higher errors, on the other hand the shapes of the obtained curves generally follow the experimental data.

The OCVs given by the model are almost the same as the experimental data. Significant differences occur with low hydrogen contents; this affects situations where hydrogen is diluted with helium and steam.

Experimental data published in [7] were used to model validation according to both temperature and electrolyte thickness. The tested cell has an area of 2 cm², and the following oxidant and fuel flows were kept constant: 550 ml/min and 300 ml/min, respectively.

The tested cell was constructed of a single layer YSZ electrolyte of thickness 8µm. Then the ionic resistance of the cell was calculated by using the following equation:

$$r_1 = \frac{\delta_{YSZ}}{\sigma_{YSZ}} + \frac{\delta_{electrodes}}{\sigma_{electrodes}} \tag{13}$$

Adequate factors of ionic conductivity for the electrolyte layer were read from Fig. 3, whereas conductivity of the electrodes was fitted for total thickness of electrodes (anode support + anode interlayer + cathode interlayer + cathode current collector) 1090µm. It should be noted that electrode losses are as significant (77%) at 800°C as they were with the previous cell design.

The influence of electrolyte layer thickness is shown in Fig. 7. Both experimental data and simulation results are presented. In general, the electrolyte influence is modelled close to the experimental data. In the model, the lower cell

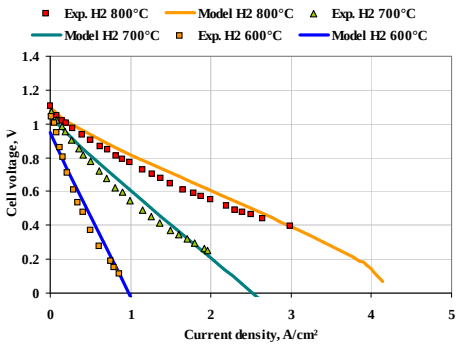

Fig. 7. Experimental and simulations data at various temperatures (experimental data taken from [7])

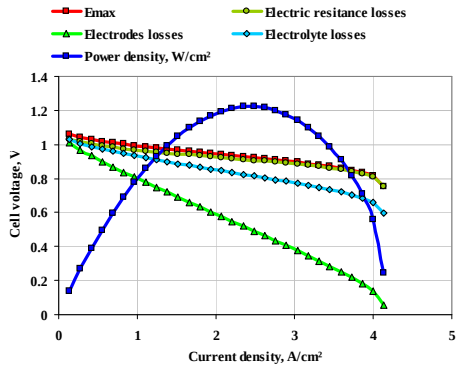

Fig. 8. Voltage-current density curve with indicated main cell losses

performances occur for the higher electrolyte thickness (see Eq. 13). The experimental data do not follow this behaviour for all data sets, e.g. electrolyte thickness of 4μm gives lower performance than 8μm.

Based on the temperature profile for the cell, the relationship for electrode conductivity as a function of temperature was obtained:

$$\sigma_{electrodes} = 1567.1 \cdot e^{\frac{-67.22}{R \cdot T}} \tag{14}$$

Equation 14 is valid only for the given cell architecture; additional investigation will be performed to find a more general relationship.

The influence of temperature on fuel cell characteristics is shown in Fig. 7. Good agreement is obtained between experimental data and simulation results. A greater difference can be seen only for OCV at 600°C, and that results from the assumption that electrical resistance (r_2) is temperature independent. The differences between the modelled voltages and experimental data are in a range of less than 10%.

Losses occurred in the cell are shown in Fig. 8. The maximum voltage calculated for partial pressures taken at both the anode and cathode outlets gives adequate shape according

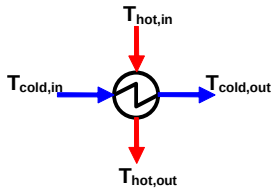

Fig. 9. Heat exchanger scheme

to both activation and concentration (diffusion) losses. The other losses are generated by the two resistances represent. The influence of electrical resistance (r_2) occurs mainly at the start of the fuel cell operation curve. From Fig. 8 it is clear that the main losses are generated across the cell electrodes (both anode and cathode). Electrolyte losses are only responsible for about 20% of total voltage loss.

The proposed model gives acceptable results for various fuel compositions. Simultaneously, dry hydrogen as well as hydrogen diluted with other components (He, H_2O, CO_2, N_2) is modelled with relatively small errors.

B. Heat exchanger

Both gas turbine and air compressor were modelled by using polytrophic efficiency based models. The polytrophic efficiencies were assumed to be constant and equal to 80%.

The heat exchanger surface is an important issue from the technical-economic point of view. At design-point the heating surface is equivalent to heat exchanger effectiveness.

Heat exchanger effectiveness is defined by the following equation:

$$\eta_{HX} = \frac{T_{hot,in} - T_{hot,out}}{T_{hot,in} - T_{cold,in}} \tag{15}$$

where: T – temperature, °C; hot – hot side of heat exchanger, $cold$ – cold side of the heat exchanger, in – inlet, out – outlet.

C. SOFC Hybrid System

A few system configurations were analyzed, starting from the SOFC only. The SOFC only represents a device which generates power by utilization of the SOFC stack only, without any additional devices. The fuel was hydrogen; there were no anode or cathode recycle flows.

All required factors of the model are listed in Table II. Those factors are needed for current density–voltage curves determination.

The laboratory scale fuel cell generates electricity at very low efficiency ~18% with a 46% fuel utilization factor. There

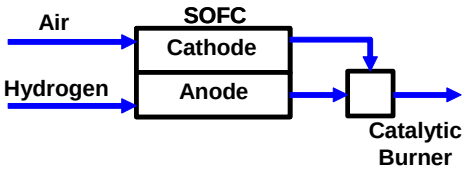

Fig. 10. The configuration of the SOFC only case

TABLE II
MAIN FACTORS USED IN THE SOFC MODEL

Factor	Value
Anode thickness, μm	1020
Cathode thickness, μm	70
Electrolyte thickness, μm	8
Electrodes ionic conductivity, S/cm	2.75
YSZ 0, S/cm	390.95
YSZ E0, kJ/mol	87.806
Electrodes 0, S/cm	1567.1
Electrodes E0, kJ/mol	67.22
Area Specific Electric Resistance, cm²/S	5.50

is a possibility to add the re-cycles on both the anode and cathode sides of the fuel cell (see Fig. 11). The anode side re-cycle gives an opportunity to work the cell with low fuel utilization factor and utilize the large amount of fuel delivered to the system at the same time. This increases system efficiency considerably. In contrast, the cathode side re-cycle has a slightly negative effect on cell voltage but helps in temperature management in the cell by elevating the cathode inlet temperature. Implementation of both the anode and cathode re-cycles to the lab-scale fuel cell increases efficiency to 37%, with a fuel utilization factor of 26%.

The first hybrid system analyzed (Case 1) consists of an SOFC stack fuelled by hydrogen, and a gas turbine subsystem. Both anode and cathode re-cycle streams were added.

The second hybrid system analyzed (Case 2) is the same configuration as Case 1, but the fuel was changed to methane.

The third hybrid system analyzed (Case 3) is similar to Case 2 but an additional heat exchanger was added. The heat exchanger is placed just after the Air Compressor and fed by the Gas Turbine outlet stream.

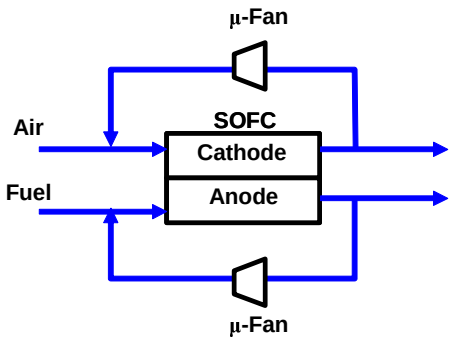

Fig. 11. The configuration of the SOFC only case with addition of anode and cathode re-cycles

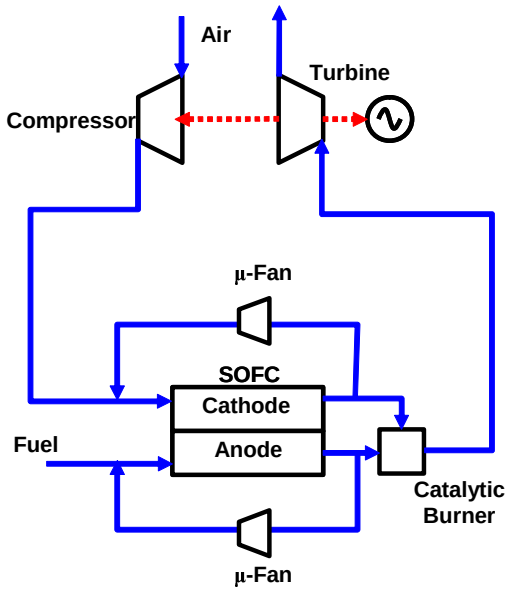

Fig. 12. The system configuration of the Case 1 and 2

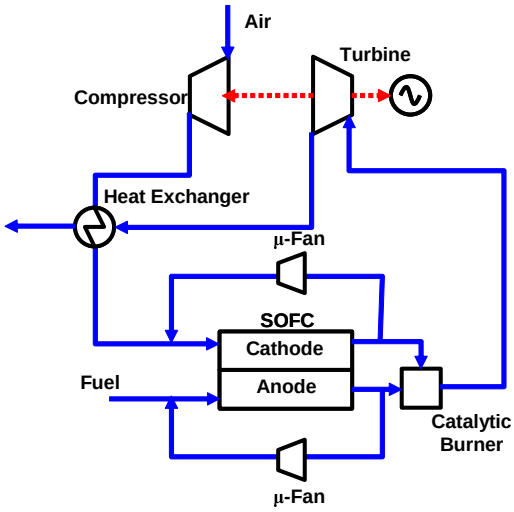

Fig. 13. The system configuration of the Case 3

D. Optimizing procedure

Objective function: System efficiency has been chosen as an optimizing objective function. Efficiency is defined by the following equation:

$$\eta_{HS} = \frac{P_{SOFC} + P_{GT} - P_C}{\dot{m}_{CH_4} \cdot LHV_{CH_4}} \tag{16}$$

where: P – power, kW; GT – Gas Turbine, C – Air Compressor, $\dot{m}$ – mass flow, LHV – Lower Heating Value.

Optimizing algorithm: Optimization calculations were performed through use of the BOX method [17], based on a

sequential search technique for the best value objective function. The method concerns nonlinear problems with nonlinear constraints. The following system parameters were subjected to an optimization process:

1) Gas Turbine pressure ratio (1–30);
2) SOFC fuel utilization factor (0–90%);
3) SOFC anode re-cycle ratio (0–90%);
4) SOFC cathode re-cycle ratio (0–90%);
5) Heat Exchanger Effectiveness (0–90%);
6) Maximum current density (2.7–10A/cm²).

Constraints: Optimizing procedures were carried out with several constraints. They mainly regarded thermal management of the installation. Cell temperature was kept at a constant 800°C and maximum Turbine Inlet Temperature (TIT) was limited to 1100°C.

III. Results

As a result, a structure (at maximum efficiency) was determined for the SOFC-GT hybrid system. This system consists of a fuel cell module, heat exchanger (regenerative) heating the air, and a gas turbine.

There were a small number of cases analyzed, the first case considered regards the SOFC only unit. The SOFC is fuelled by dry hydrogen only. This case is used as the reference case for the next hybrid system analysis. Case 1 is based on the simplest hybrid system which consists of the SOFC unit, gas turbine, and air compressor. Case 1 is still fuelled by hydrogen only. This configuration can reach an efficiency level of 57%. The optimum pressure ratio of the gas turbine subsystem is 13 with TIT of 1100°C.

Hydrogen is unavailable in uncombined form and a more practical fuel is Natural Gas. Natural Gas consists mainly of methane. The hybrid system in Case 2 has the same configuration as Case 1, but the fuel has been changed to methane. The internal reforming reactions convert the thermal energy generated inside the SOFC to the form of fuel by decomposing methane and steam to hydrogen. This raises efficiency to 63%. Other system parameters are: gas turbine pressure ratio of 19 with TIT of 1100°C.

An adequate heat exchanger can increase efficiency by recovering part of the gas turbine outlet heat. In Case 3, the heat exchanger is placed between the air compressor and the SOFC. This solution increases efficiency to 66% and decreases the gas turbine pressure ratio to 8.2. TIT is still very high at 1100°C. The volume of the heat exchanger is relatively large, because 90% effectiveness is needed.

TABLE III
Main parameters of the analyzed cases

Parameter	Case					
	SOFC	SOFC	1	2	3	4
Fuel	H_2	H_2	H_2	CH_4	CH_4	CH_4
Efficiency, %	18	37	57	63	66	68
Fuel Utilization Factor, %	46	26	21	27	26	34
Anode Re-cycle, %	0	90	90	90	85	90
Cathode Re-cycle, %	0	70	40	43	43	42
i_{max}, A/cm²	5.4	5.4	5.4	5.4	5.4	2.77
TIT, °C	-	-	1100	1100	1100	1025
GT Pressure Ratio	-	-	13	19	8.2	9.6
s/c ratio	-	-	-	4.1	2.5	5
Heat Exchanger Effectiveness, %	-	-	-	-	90	62

The last case analyzed (Case 4) has the same fuel and system configuration as Case 3. The difference is the cell area, which is twice as big but raises efficiency only by 2%. Detailed parameters for all analyzed cases are listed in Table III.

IV. Discussion

The obtained results show that the hybrid system gives very high levels of efficiency. The hydrogen fuelled laboratory scale SOFC generates electricity at 18% efficiency. Efficiency can be raised to 37% by the addition of both the anode and cathode re-cycles. Apart from the increase in efficiency, those re-cycles are required to bring about a proper heat balance of the cell.

Simple addition of a gas turbine subsystem can raise efficiency to 57%. The efficiency increase is mostly caused by the anode re-cycle process, which allows the cell to be worked at a low fuel utilization factor (21%) while simultaneously utilizing 75% of the fuel delivered to the system. The power generated by the gas turbine subsystem represents about 30% of the total system power.

Changing the fuel type, methane instead of hydrogen, results in efficiency increasing to 63%. This is mostly caused by internal steam reforming reactions of methane, causing process heat recuperation.

The next upgrade of the system is the addition of a heat exchanger, which is placed between the fuel cell stack and the air compressor. The heat exchanger is fed by the gas turbine outlet stream. This solution increases efficiency to 66%.

Increasing the fuel cell area by a factor of two causes efficiency to rise by only by 2%. Any technical analysis must be performed together with an economics based analysis

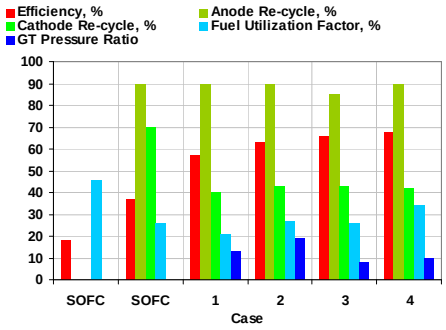

Fig. 14. Main parameters of the analyzed cases

to obtain the most favourable system configuration from the financial point of view.

There are two re-cycle streams: on the anode and the cathode sides. The cathode side re-cycle only helps the heat balance of the fuel cell stack. It does not increase efficiency and can be avoided. The anode side re-cycle is crucial to obtain high efficiency and should be kept as high as possible.

V. Conclusions

The mathematical model of SOFC for various fuel compositions is proposed. The model was based on a combination of electric laws, gas flow relationships, solid materials properties, and electro-chemical correlations. The presented model is very stable and can be used for both simulations and optimization procedures. During those procedures in all cases physical results will be generated (e.g. cell voltage is always lower than 1.2V and so on). In contrast, models based on the Butler-Volmer equations are very sensitive to input parameters and frequently generate non-physical results (e.g. for $i = 0$ A/cm^2).

The presented model was validated for various fuel mixtures over a relatively wide range of parameters. The model is characterized by the lowest number of factors needed. Separation is made between the "design-point" and "off-design operation" modes. Comparison with experimental data is shown and commented.

A small number of different hybrid systems were analyzed and described. It should be noted that the fuel cell which works inside the hybrid system has quite different working conditions and parameters from the cell used in laboratory scale experiments. A appropriate procedure for scaling-up the cell is a crucial issue for obtaining high efficiencies.

Power generated by the gas turbine subsystem is responsible for about 30% of total power generated. The gas turbine pressure ratios are on average at level 8–10, and are technically possible for implementation. The optimum pressure ratio is correlated with TIT, which was limited to 1100°C. Lower values of TIT will cause lower system efficiency but can be easier for implementation in practical situations.

The anode re-cycle process is crucial for obtaining high efficiency. This can be accomplished by either an ejector or a fan (μ-fan). A large part of the anode outlet stream must be turned back to the anode inlet. Those gases are relatively hot (800°C) and are necessary for internal steam reforming of methane. Too small an amount of steam can destroy the fuel cell very quickly due to carbon deposition. The use of the μ-fan is preferred because it makes the re-cycle process independent of the amount of fuel delivered.

References

[1] S. Kakac, A. Pramuanjaroenkij, and X. Zhou, "A review of numerical modeling of solid oxide fuel cells," *International Journal of Hydrogen Energy*, vol. 32, no. 7, pp. 761–786, 2007.

[2] C. O. Colpan, I. Dincer, and F. Hamdullahpur, "A review on macro-level modeling of planar solid oxide fuel cells," *International Journal Of Energy Research*, vol. 32, pp. 336–355, 2008.

[3] F. Zabihian and A. Fung, "A review on modeling of hybrid solid oxide fuel cell systems," *International Journal of Engineering*, vol. 3, pp. 85–119, 2009.

[4] Hyprotech Corporation, *HYSYS.Plant Steady State Modelling*, 1998.

[5] J. Milewski, K. Świrski, M. Santarelli, and P. Leone, *Advanced Methods of Solid Oxide Fuel Cell Modeling*. Springer-Verlag London Ltd., 1st edition ed., March 2011.

[6] Y. Jiang and A. V. Virkar, "Fuel composition and diluent effect on gas transport and performance of anode-supported sofcs," *Journal of The Electrochemical Society*, vol. 150, no. 7, pp. A942–A951, 2003.

[7] F. Zhao and A. Virkar, "Dependence of polarization in anode-supported solid oxide fuel cells on various cell parameters," *Journal of Power Sources*, vol. 141, no. 1, pp. 79 – 95, 2005.

[8] A. Virkar, "Theoretical analysis of the role of interfaces in transport through oxygen ion and electron conducting membranes," *Journal of Power Sources*, vol. 147, no. 1–2, pp. 8–31, 2005.

[9] T. Ishihara, T. Shibayama, M. Honda, H. Nishiguchi, and Y. Takita, "Solid oxide fuel cell using co doped la(sr)ga(mg)o3 perovskite oxide with notably high power density at intermediate temperature," *Chemical communications*, vol. 13, pp. 1227–1228, 1999.

[10] Z. Cai, T. Lan, S. Wang, and M. Dokiya, "Supported Zr(Sc)O2 SOFCs for reduced temperature prepared by slurry coating and co-firing," *Solid State Ionics*, vol. 152-153, no. 1, pp. 583–590, 2002.

[11] B. Madsen and S. Barnett, "Effect of fuel composition on the performance of ceramic-based solid oxide fuel cell anodes," *Solid State Ionics*, vol. 176, pp. 2545–2553, 2005.

[12] D. Young, A. Sukeshini, R. Cummins, H. Xiao, M. Rottmayer, and T. Reitz, "Ink-jet printing of electrolyte and anode functional layer for solid oxide fuel cells," *Journal of Power Sources*, vol. 184, no. 1, pp. 191–196, 2008.

[13] W. Zhou, H. Shi, R. Ran, R. Cai, Z. Shao, and W. Jin, "Fabrication of an anode-supported yttria-stabilized zirconia thin film for solid-oxide fuel cells via wet powder spraying," *Journal of Power Sources*, vol. 184, no. 1, pp. 229–237, 2008.

[14] J. Ding and J. Liu, "An anode-supported solid oxide fuel cell with spray-coated yttria-stabilized zirconia (ysz) electrolyte film," *Solid State Ionics*, vol. 179, pp. 1246–1249, 2008.

[15] Z. Yao, Z. Chunming, R. Ran, R. Cai, Z. Shao, and D. Farrusseng, "A new symmetric solid oxide fuel cell with La0.8Sr0.2Sc0.2Mn0.8O3-Δ perovskite oxide as both the anode and cathode," *Acta Materialia*, vol. 57, no. 4, pp. 1665–1175, 2009.

[16] H. Park and A. Virkar, "Bimetallic (ni-fe) anode-supported solid oxide fuel cells with gadolinia-doped ceria electrolyte," *Journal of Power Sources*, vol. 186, pp. 133–137, 2009.

[17] M. Box, "A new method of constrained optimization and a comparison with other methods," *The Computer Journal*, vol. 8, pp. 42–52, 1965.